

# Highly Sensitive and Fast-Responding Ethanol Sensor using Au Doped-In<sub>2</sub>O<sub>3</sub> Hollow Spheres

Seong-Young Jeong<sup>1,+</sup>

## Abstract

Pure and 0.3 wt% Au-doped In<sub>2</sub>O<sub>3</sub> hollow spheres were synthesized via ultrasonic spray pyrolysis of droplets containing an In-source and sucrose in air and their gas sensing characteristics to 1 ppm ethanol, 1 ppm toluene, 1 ppm xylene, 2 ppm nitrogen dioxide (NO<sub>2</sub>), and 30 ppm carbon monoxide (CO) were measured at 400 – 450°C. The pure In<sub>2</sub>O<sub>3</sub> hollow spheres exhibited relatively low gas responses and sluggish recovery kinetics. In contrast, the doping of Au into In<sub>2</sub>O<sub>3</sub> hollow spheres significantly increased the gas response (S= resistance ratio) to 1 ppm ethanol (S= 20.6) at 400°C with low cross-responses (S = 1.3-8.8) to other interference gases. Furthermore, the hollow spherical morphology of In<sub>2</sub>O<sub>3</sub> provides a large surface area and facilitates rapid gas diffusion, resulting in fast response and recovery times. The sensor exhibited excellent performance with a low detection limit of 1.6 ppb. These findings indicate that the Au-In<sub>2</sub>O<sub>3</sub> hollow spheres are promising candidates for advanced ethanol-sensing applications, particularly in breath-alcohol monitoring for ignition interlock devices.

**Keywords:** Gas sensors, Oxide semiconductors, In<sub>2</sub>O<sub>3</sub>, Ethanol, Hollow spheres

## 1. INTRODUCTION

As public awareness of the dangers associated with drinking increases, the importance of breath-alcohol (*e.g.*, ethanol) monitoring has attracted considerable research attention. Interest has also been growing in noncontact alcohol detection systems for vehicle ignition control [1,2]. These systems are designed to detect trace amounts of alcohol in the breath, sweat, or skin respiration of the driver within a few seconds of the vehicle door being closed, thereby enabling automated control over the ignition system. Thus, detection systems can reduce the social and economic damage caused by driving under the influence (DUI) of alcohol by integrating various detectors near the driver's seat, which can accurately detect alcohol consumption and if found, inhibit vehicle operation.

As candidate components for alcohol detection systems, metal oxide-based semiconductors have been widely studied because of their high response, cost-effectiveness, and easy integration

into compact devices [3-12]. This is particularly advantageous for detecting alcohol levels in a driver's breath, which correlates with the blood alcohol concentration. This allows assessment of whether the legal limit for alcohol consumption (typically hundreds of ppm) has been exceeded. However, several technical challenges must be addressed before implementing such systems. The concentration of alcohol in the driver's breath or emitted from the skin is often extremely low and diluted by the surrounding air, resulting in trace alcohol levels of only a few ppm. This dilution poses significant challenges for alcohol detection.

Accordingly, the sensors utilized in such noncontact systems should be extremely sensitive for detecting sub-ppm alcohol levels. Furthermore, alcohol should be discriminated from other volatile organic compounds (VOCs) such as toluene and xylene, which are commonly present in vehicle interiors, and from other pollutants such as carbon monoxide and nitrogen oxides from fuel combustion [13-15]. These interfering gases could potentially lead to gas detection malfunctions; therefore, the sensor should have high selectivity for ethanol. Additionally, the sensor should afford rapid response and recovery times, ideally within a few seconds, to avoid inconveniencing drivers.

In this study, an ethanol sensor with high gas response, selectivity, and high response speed was designed using Au-In<sub>2</sub>O<sub>3</sub> hollow spheres. Doping 0.3 wt% Au into In<sub>2</sub>O<sub>3</sub> significantly increased the gas responses and selectivity, and the hollow

<sup>1</sup>Division of Advanced Materials Engineering, Kongju National University Cheonan, Chungnam 31080, Republic of Korea

<sup>+</sup>Corresponding author: syjeong@kongju.ac.kr

(Received: Aug. 19, 2024, Revised: Aug. 28, 2024, Accepted: Sep. 2, 2024)

This is an Open Access article distributed under the terms of the Creative Commons Attribution Non-Commercial License (<https://creativecommons.org/licenses/by-nc/3.0/>) which permits unrestricted non-commercial use, distribution, and reproduction in any medium, provided the original work is properly cited.

morphology facilitated the rapid recovery to ethanol. In addition, the promising potential of the Au-In<sub>2</sub>O<sub>3</sub> hollow spheres as breath-alcohol sensing materials was demonstrated by their ultrahigh response to gases, even at sub-ppm ethanol levels

## 2. EXPERIMENT

### 2.1 Preparation of pure In<sub>2</sub>O<sub>3</sub> and Au-In<sub>2</sub>O<sub>3</sub> microspheres

Au-doped In<sub>2</sub>O<sub>3</sub> hollow spheres were synthesized using ultrasonic spray pyrolysis (Fig. 1). The process involved dissolving indium (III) nitrate hydrate (0.05 M, In(NO<sub>3</sub>)<sub>3</sub>·xH<sub>2</sub>O, 99.999%, Sigma–Aldrich, USA) and sucrose (0.15 M, C<sub>12</sub>H<sub>22</sub>O<sub>11</sub>, 99.5%, Sigma–Aldrich, USA) in 600 mL of distilled water. After stirring for 10 minutes at room temperature, an appropriate amount of gold (III) chloride ([Au/In] = 0.3 wt%, AuCl<sub>3</sub>, 99.99% trace metals basis, Sigma–Aldrich, USA) was added to the solution. The droplets were nebulized by ultrasonic generators and directly moved into a high-temperature (900°C) quartz reactor by air (flow rate = 5 L min<sup>-1</sup>). The resulting powder was collected using a Teflon filter. The morphology and phase of the hollow structures were analyzed using field-emission scanning electron microscopy (FE-SEM, S-4300 Hitachi Co., Ltd., Japan) and X-ray diffraction (XRD, Rigaku Model/MAX-2500, Source: CuKα).

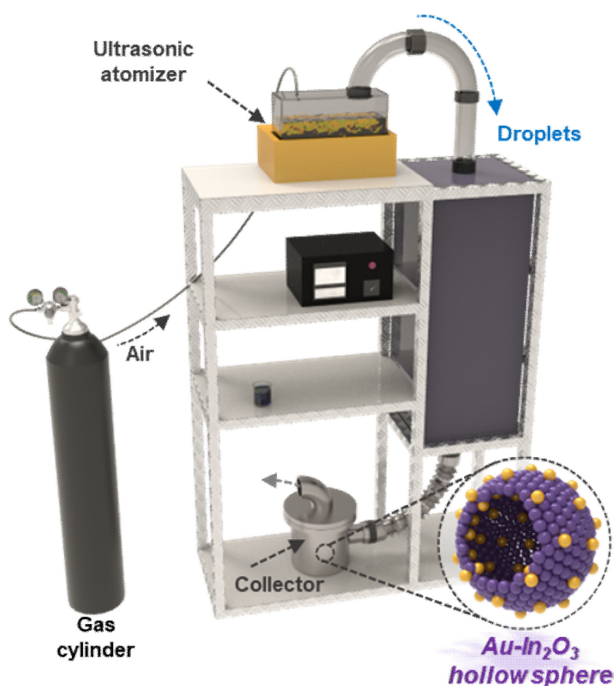


Fig. 1. Synthesis of pure Au-In<sub>2</sub>O<sub>3</sub> hollow spheres

### 2.2 Gas-sensing characteristics

The prepared powders were dispersed in distilled water, and the resulting slurry was drop-coated onto a sensor substrate (dimensions: 1.5 × 1.5 mm<sup>2</sup>) with two gold electrodes. All sensors were then heated to 500°C for 2 h to remove the hydroxyl groups and stabilize the sensor. The sensors were then placed inside a custom-designed quartz tube (volume: 1.5 cm<sup>3</sup>). Gas-sensing measurements were performed in a dry air atmosphere with periodic exposure to the target gases. Dry air and analyte gases were introduced at a constant flow rate of 500 cm<sup>3</sup>/min. The sensor resistance was measured using a picoammeter (Model 6487; Keithley, Tektronix, Inc., USA). The sensor temperature was controlled by applying a voltage to the Ru microheater positioned at the base of the sensor substrate using a direct current (DC) power supply (E3646A, Keysight Technologies, Inc., USA).

## 3. RESULTS AND DISCUSSION

### 3.1 Materials characterization

Fig. 2 shows the SEM images of pure In<sub>2</sub>O<sub>3</sub> and Au-doped In<sub>2</sub>O<sub>3</sub> hollow spheres. Both the pure In<sub>2</sub>O<sub>3</sub> and Au-doped In<sub>2</sub>O<sub>3</sub> powders respectively exhibited spherical morphologies, with average diameters of 0.84 ± 0.42 μm and 0.95 ± 0.43 μm. Hollow morphologies were frequently observed in all samples (arrow in Fig. 2 (a) and (b)), which was further confirmed by the broken spheres in the high-magnification SEM images (Fig. 2 (b)). This suggests that both In<sub>2</sub>O<sub>3</sub>-based hollow spheres exhibit highly gas-accessible structures:

The Au-In<sub>2</sub>O<sub>3</sub> hollow spheres were further examined using XRD, which revealed that they exhibited a cubic phase (ICDD #06-0416) (Fig. 3). No Au-related peaks appeared in the XRD pattern, probably because of the X-ray diffractometer's low detection limit. The crystallite size of the Au-In<sub>2</sub>O<sub>3</sub> hollow spheres

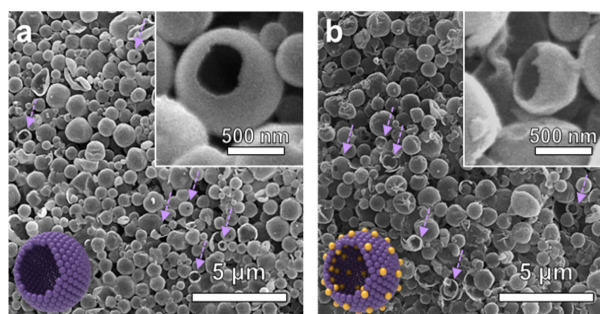


Fig. 2. Scanning electron microscopy images of (a) pure In<sub>2</sub>O<sub>3</sub> and (b) Au-doped In<sub>2</sub>O<sub>3</sub> hollow spheres

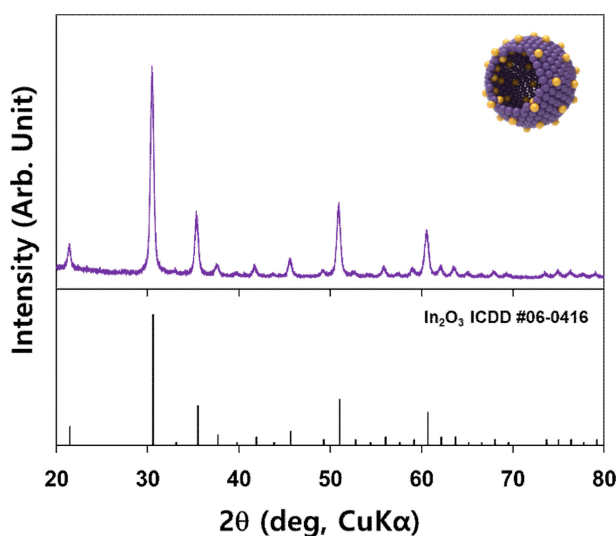


Fig. 3. X-ray diffraction pattern of Au-In<sub>2</sub>O<sub>3</sub> hollow spheres.

was determined to be  $16.5 \pm 1.8$  nm according to Scherrer's equation. However, further investigations are required to elucidate the Au-related phase index and demonstrate its incorporation into In<sub>2</sub>O<sub>3</sub>.

### 3.2 Gas sensing characteristics and discussion

The gas-sensing characteristics of the sensors using pure In<sub>2</sub>O<sub>3</sub> and Au-In<sub>2</sub>O<sub>3</sub> hollow spheres in the presence of 1 ppm ethanol, 1 ppm toluene, 1 ppm xylene, 2 ppm NO<sub>2</sub>, and 30 ppm CO were investigated at 400 – 450°C (Fig. 4). All sensors exhibited the typical characteristics of n-type metal-oxide chemiresistors. Their measured resistance decreased upon exposure to a reducing gas, increased when exposed to an oxidizing gas, and returned to its original value when subsequently exposed to air. Therefore, the gas response (S) was defined using Eq. (1):

$$S = R_a/R_g \text{ or } R_g/R_a \quad (1)$$

where  $R_a$  is the resistance of the sensor in air and  $R_g$  is the resistance of the analyte gas.

For the sensor using pure In<sub>2</sub>O<sub>3</sub> hollow spheres, the response to 1 ppm of ethanol was higher than those of other analyte gases over the entire sensing temperature ranges (400 – 450°C) (Fig. 4 (a)), which is consistent with the typical gas-sensing characteristics of pure In<sub>2</sub>O<sub>3</sub> sensors [16–19]. However, it is difficult to be highly selective in detecting ethanol because the response is comparable to that of other interfering gases. This trend toward a reduced ethanol response was predominant at elevated temperatures. This indicated that pure In<sub>2</sub>O<sub>3</sub> was insufficient for the selective detection of a given gas.

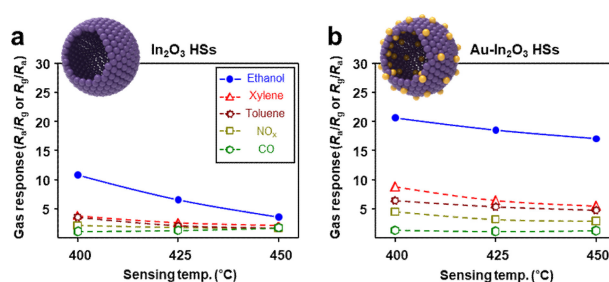


Fig. 4. Gas sensing properties of the (a) pure In<sub>2</sub>O<sub>3</sub> and (b) Au-doped In<sub>2</sub>O<sub>3</sub> hollow spheres (concentration of the analyte gas: 1 ppm of ethanol, 1 ppm of xylene, 1 ppm of toluene, 2 ppm of NO<sub>x</sub>, 30 ppm of CO; temperature range: 400 – 450°C).

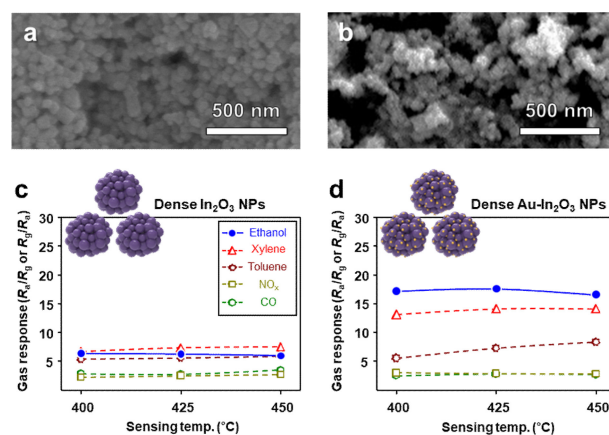


Fig. 5. SEM images of (a) pure In<sub>2</sub>O<sub>3</sub> and (b) Au-doped In<sub>2</sub>O<sub>3</sub> nanoparticles. Gas sensing properties of the (a) pure In<sub>2</sub>O<sub>3</sub> and (b) Au-doped In<sub>2</sub>O<sub>3</sub> nanoparticles (concentration of the analyte gas: 1 ppm of ethanol, 1 ppm of xylene, 1 ppm of toluene, 2 ppm of NO<sub>x</sub>, 30 ppm of CO; temperature range: 400 – 450°C).

In contrast, doping with Au significantly changes the gas-sensing performance. The response to ethanol increased significantly over the entire sensing temperature range, enabling highly selective and sensitive detection. The response of the sensor using Au-In<sub>2</sub>O<sub>3</sub> hollow spheres to 1 ppm ethanol ( $S = 20.6$ ) was significantly higher than that of 1 ppm xylene ( $S = 8.8$ ), 1 ppm toluene ( $S = 6.4$ ), 2 ppm NO<sub>x</sub> ( $S = 1.3$ ), and 30 ppm CO ( $S = 4.5$ ) at 400°C (Fig. 4 (b)).

To emphasize the highly sensitive and selective ethanol detection properties of the Au-In<sub>2</sub>O<sub>3</sub> hollow spheres, we further investigated their gas-sensing characteristics using commercially available In<sub>2</sub>O<sub>3</sub> and Au-In<sub>2</sub>O<sub>3</sub> nanoparticles (Fig. 5 (a) and (b)). The sensor using pure In<sub>2</sub>O<sub>3</sub> commercial nanoparticles showed relatively low gas responses to all the analyte gases over a broad temperature range (Fig. 5 (c)). In contrast, the overall response increased significantly with Au doping (Fig. 5 (d)). However, this approach was not highly selective for ethanol. A similar response

to ethanol may be attributed to the oxidation of highly reactive ethanol and the gas reforming (*e.g.*, partial oxidation) of less reactive compounds such as xylene and toluene as they pass through the gas-sensing film comprising dense In<sub>2</sub>O<sub>3</sub> nanoparticles. These findings indicate that Au doping of In<sub>2</sub>O<sub>3</sub> significantly improves the gas response; however, the dense nanostructure hinders selective ethanol detection.

The significant increase in the gas response and selectivity arising from In<sub>2</sub>O<sub>3</sub> being doped with Au can be understood in relation to the variation in the charge carrier concentration, catalytic activation, and oxygen adsorption. When a fixed number of charge carriers (*e.g.*, electrons) is injected into the sensing materials through the interaction between the sensor surface and analyte gases, materials with a lower charge carrier concentration tend to exhibit higher chemiresistive variation. Previous studies have demonstrated that doping with Au results in charge carrier transfer from In<sub>2</sub>O<sub>3</sub> to Au because Au has a higher work function (5.1 eV) than In<sub>2</sub>O<sub>3</sub> (4.15 eV) (*i.e.*, electronic sensitization) [20]. Furthermore, it has also been reported that Au facilitates oxygen dissociation, thereby enhancing oxygen adsorption on the gas-sensing surface. Therefore, the gas response to ethanol can be increased by catalytically sensitizing Au in the gas-sensing reaction (*i.e.*, chemical sensitization) [21].

To examine both the electronic and chemical sensitization effects, the  $R_a$  value of the sensors was measured (Fig. 6 (a)). The  $R_a$  values of the pure In<sub>2</sub>O<sub>3</sub> hollow spheres ranged from 32.2 (at 400 °C) to 12.5 k $\Omega$  (at 450 °C), which substantially increased (approximately 2 times) with Au doping. This is consistent with previous reports on the enhancement of the gas response to ethanol in n-type oxide semiconductors by Au doping, including Au-SnO<sub>2</sub> hollow spheres [21], Au@SnO<sub>2</sub> hierarchical hollow spheres [22], Au-In<sub>2</sub>O<sub>3</sub> nanofibers [23], Au-modified ZnO microwires [24], and Au/Pd-doped ZnO nanorods [25].

Fast response and recovery kinetics are important for breath-alcohol sensing applications. Therefore, the 90% response and recovery times ( $\tau_{res}$  and  $\tau_{recov}$ ), representing the time required to achieve 90% of the resistance change upon exposure to ethanol and air, respectively, were calculated from the dynamic gas-sensing transients. All sensors exhibited similar  $\tau_{res}$  values (2 – 10 s) upon exposure to 1 ppm ethanol (Fig. 6 (a)), but their  $\tau_{recov}$  values differed significantly (Fig. 6 (b)). For example, the commercial Au-In<sub>2</sub>O<sub>3</sub> nanoparticle sensor evidenced a prolonged recovery time ( $\tau_{recov} = 938 - 380$  s at 400 – 450°C), whereas significantly reduced  $\tau_{recov}$  values were achieved with the In<sub>2</sub>O<sub>3</sub> (368 – 200 s at 400 – 450°C) and Au-In<sub>2</sub>O<sub>3</sub> hollow spheres (164 – 295 s at 400 – 450°C). This finding suggests that the hollow

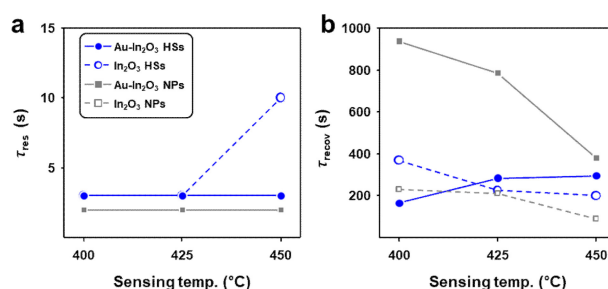


**Fig. 6.** (a) 90% response time ( $\tau_{res}$ ) and (b) 90% recovery time ( $\tau_{recov}$ ) of the pure In<sub>2</sub>O<sub>3</sub> hollow sphere, Au-In<sub>2</sub>O<sub>3</sub> hollow sphere, pure In<sub>2</sub>O<sub>3</sub> nanoparticle, and Au-In<sub>2</sub>O<sub>3</sub> nanoparticle sensors at 400 – 450°C.

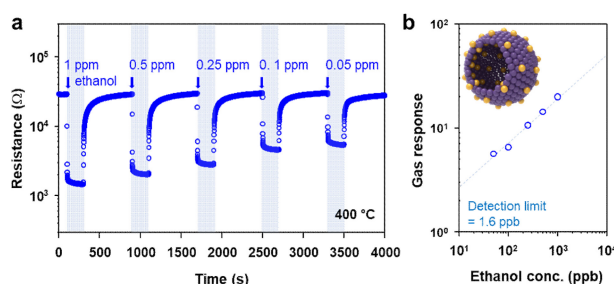


**Fig. 7.** (a) Dynamic gas-sensing transients of the Au-In<sub>2</sub>O<sub>3</sub> hollow spheres exposed to 0.1–1 ppm ethanol at 400°C; (b) gas response as a function of ethanol concentration.

morphology is advantageous for achieving the highly sensitive, selective, and rapid detection of ethanol, which may offer significant advantages for ethanol-sensing applications.

Fig. 7 shows the gas responses of the Au-In<sub>2</sub>O<sub>3</sub> hollow spheres to 0.05–1 ppm ethanol at 400°C (Fig. 7 (a)). The detection limit for ethanol was calculated to be as low as 1.6 ppb when  $R_a/R_g > 1.2$  was used as the sensing criterion (Fig. 7 (b)). From this perspective, the proposed sensor can be used for breath-alcohol monitoring.

## 4. CONCLUSION

In this study, we successfully developed a highly sensitive and selective ethanol sensor using Au-doped In<sub>2</sub>O<sub>3</sub> hollow spheres. The doping of Au into In<sub>2</sub>O<sub>3</sub> significantly enhanced the gas response and selectivity, particularly towards ethanol, thereby demonstrating the efficacy of Au doping in modifying the electronic and chemical properties of the sensor material. The hollow spherical morphology of In<sub>2</sub>O<sub>3</sub> further contributes to the rapid response and recovery times, making these sensors suitable for real-time ethanol-detection applications, such as breath-alcohol monitoring.

The sensor exhibited a low detection limit of 1.6 ppb. These findings indicate that Au-In<sub>2</sub>O<sub>3</sub> hollow spheres are promising candidates for the development of advanced ethanol-sensing technologies with potential applications in public safety and health monitoring. Future work will focus on further optimizing the sensor design and exploring the underlying mechanisms to enhance detection performance and expand the range of detectable gases.

## ACKNOWLEDGMENT

This work was supported by grants (No. RS-2024-00454367) from the National Research Foundation (NRF) of Korea, funded by the Government of Korea (MSIT). This work was also supported by the Human Resource Development Program for Industrial Innovation (P0017012), funded by the Ministry of Trade, Industry, and Energy (MOTIE), Korea.

## REFERENCES

- [1] L. Tao, P. Tang, J. Hu, and Y. Zhang, "The alcohol lock built on carbon-based field-effect transistor sensor with Pd/ZnO floating gate structure used for drunk driving surveillance", *Sens. Actuators B Chem.*, Vol. 419, No. 15, p. 136393, 2024.
- [2] X.-H. Ma, H.-Y. Li, S.-H. Kweon, S.-Y. Jeong, J.-H. Lee, and S. Nahm, "Highly Sensitive and Selective PbTiO<sub>3</sub> Gas Sensors with Negligible Humidity Interference in Ambient Atmosphere", *ACS Appl. Mater. Interfaces*, Vol. 11, No. 5, pp. 5240-5246, 2019.
- [3] N. Yamazoe, "Toward Innovations of Gas Sensor Technology", *Sens. Actuator B Chem.*, Vol. 108, No. 1-2, pp. 2-14, 2005.
- [4] F. Röck, N. Barsan, and U. Weimar, "Electronic nose: current status and future trends", *Chem. Rev.*, Vol. 108, No.2, pp. 705-725, 2008.
- [5] A. Kolmakov, Y. Zhang, G. Cheng, and M. Moskovits, "Detection of CO and O<sub>2</sub> Using Tin Oxide Nanowire Sensors", *Adv. Mater.*, Vol. 15, No. 12, pp. 997-1000, 2003.
- [6] A. Sanger, S. B. Kang, M. H. Jeong, M. J. Im, I. Y. Choi, C. U. Kim, H. Lee, Y. M. Kwon, J. M. Baik, H. W. Jang, and K. J. Choi, "Morphology-Controlled Aluminum-Doped Zinc Oxide Nanofibers for Highly Sensitive NO<sub>2</sub> Sensors with Full Recovery at Room Temperature", *Adv. Sci.*, Vol. 5, No. 9, pp. 1800816(1)-1800816(8), 2018.
- [7] J. Shin, S.-J. Choi, I. Lee, D.-Y. Youn, C. O. Park, J.-H. Lee, H. L. Tuller, and I.-D. Kim, "Thin-Wall Assembled SnO<sub>2</sub> Fibers Functionalized by Catalytic Pt Nanoparticles and their Superior Exhaled-Breath-Sensing Properties for the Diagnosis of Diabetes", *Adv. Funct. Mater.*, Vol. 23, No. 19, pp. 2357-2367, 2013.
- [8] Y. G. Song, J. Y. Park, J. M. Suh, Y.-S. Shim, S. Y. Yi, H. W. Jang, S. Kim, J. M. Yuk, B.-K. Ju, and C.-Y. Kang, "Heterojunction Based on Rh-Decorated WO<sub>3</sub> Nanorods for Morphological Change and Gas Sensor Application Using the Transition Effect", *Chem. Mater.*, Vol. 31, No. 1, pp. 207-215, 2019.
- [9] S. Park, S. Kim, G.-J. Sun, and C. Lee, "Synthesis, Structure, and Ethanol Gas Sensing Properties of In<sub>2</sub>O<sub>3</sub> Nanorods Decorated with Bi<sub>2</sub>O<sub>3</sub> Nanoparticles", *ACS Appl. Mater. Interfaces*, Vol. 7, No. 15, pp. 8138-8146, 2015.
- [10] J.-H. Lee, "Gas Sensors using Hierarchical and Hollow Oxide Nanostructures: Overview", *Sens. Actuators B Chem.*, Vol. 140, No. 1, pp. 319-336, 2009.
- [11] S.-Y. Jeong, J.-S. Kim, and J.-H. Lee, "Rational Design of Semiconductor-Based Chemiresistors and Their Libraries for Next-Generation Artificial Olfaction", *Adv. Mater.*, Vol. 32, No. 51, pp. 2002075(1)-2002075(47), 2020.
- [12] S.-Y. Jeong, "Recent Advances and Trends in Filters for Highly Selective Metal Oxide Gas Sensors", *J. Sens. Sci. Technol.*, Vol. 33, No. 1, pp. 48-55, 2024.
- [13] Y. Berkay, S.-B. Lee, and J. Lee, "Temporal variations of volatile organic compounds inside the cabin of a new electric vehicle under different operation modes during winter using proton transfer reaction time-of-flight mass spectrometry", *J. Hazard. Mater.*, Vol. 453, p. 131368, 2023.
- [14] F. A. Esteve-Turrillas, A. Pastor, and M. d. Guardia, "Assessing air quality inside vehicles and at filling stations by monitoring benzene, toluene, ethylbenzene and xylenes with the use of semipermeable devices", *Anal. Chim. Acta*, Vol. 593, No. 1, pp. 108-116, 2007.
- [15] T. L. H. Doan, J.-Y. Kim, J.-H. Lee, L. H. T. Nguyen, Y. T. Dang, K.-B. T. Bui, A. T. T. Pham, A. Mirzaei, T. B. Phan, and S. S. Kim, "Preparation of n-ZnO/p-Co<sub>3</sub>O<sub>4</sub> heterojunctions from zeolitic imidazolate frameworks (ZIF-8/ZIF-67) for sensing low ethanol concentrations", *Sens. Actuator B Chem.*, Vol. 348, p. 130684, 2021.
- [16] C. Zhang, Y. Huan, Y. Li, Y. Luo, and M. Debligny, "Low concentration isopropanol gas sensing properties of Ag nanoparticles decorated In<sub>2</sub>O<sub>3</sub> hollow spheres", *J. Adv. Ceram.*, Vol. 11, No. 3, pp. 379-391, 2022.
- [17] C.-S. Lee, H.-Y. Li, B.-Y. Kim, Y.-M. Jo, H.-G. Byun, I.-S. Hwang, F. Abdel-Hady, A. A. Wazzan, and J.-H. Lee, "Discriminative detection of indoor volatile organic compounds using a sensor array based on pure and Fe-doped In<sub>2</sub>O<sub>3</sub> nanofibers", *Sens. Actuator B Chem.*, Vol. 285, pp. 193-200, 2019.
- [18] X. Yang, H. Fu, Y. Tian, Q. Xie, S. Xiong, D. Han, H. Zhang, and X. An, "Au decorated In<sub>2</sub>O<sub>3</sub> hollow nanospheres: A novel sensing material toward amine", *Sens. Actuator B Chem.*, Vol. 296, pp. 126696(1)-126696(10), 2019.
- [19] J. Ma, H. Fan, W. Zhang, J. Sui, C. Wang, M. Zhang, N. Zhao, A. K. Yadav, W. Wang, W. Dong, and S. Wang, "High sensitivity and ultra-low detection limit of chlorine gas sensor based on In<sub>2</sub>O<sub>3</sub> nanosheets by a simple template method", *Sens. Actuator B Chem.*, Vol. 305, p. 127456, 2020.
- [20] J. Fang, Z.-H. Ma, J.-J. Xue, X. Chen, R.-P. Xiao, and J.-M.

- Song, "Au doped In<sub>2</sub>O<sub>3</sub> nanoparticles: Preparation, and their ethanol detection with high performance", *Mater. Sci. Semicond. Process.*, Vol. 146, p. 106701, 2022.
- [21] S.-W. Park, S.-Y. Jeong, J.-W. Yoon, and J.-H. Lee, "General Strategy for Designing Highly Selective Gas-Sensing Nanoreactors: Morphological Control of SnO<sub>2</sub> Hollow Spheres and Configurational Tuning of Au Catalysts", *ACS Appl. Mater. Interfaces*, Vol. 12, No. 46, pp. 51607-51615, 2020.
- [22] Y. Liu, X. Li, Y. Wang, X. Li, P. Cheng, Y. Zhao, F. Dang, and Y. Zhang, "Hydrothermal synthesis of Au@SnO<sub>2</sub> hierarchical hollow microspheres for ethanol detection", *Sens. Actuator B Chem.*, Vol. 319, p. 128299, 2020.
- [23] X. Xu, H. Fan, Y. Liu, L. Wang, and T. Zhang, "Au-loaded In<sub>2</sub>O<sub>3</sub> nanofibers-based ethanol micro gas sensor with low power consumption", *Sens. Actuator B Chem.*, Vol. 160, No. 1, pp. 713-719, 2011.
- [24] A. L. Zou, Y. Qiu, J. J. Yu, B. Yin, G. Y. Cao, H. Q. Zhang, and L. Z. Hu, "Ethanol sensing with Au-modified ZnO microwires", *Sens. Actuator B Chem.*, Vol. 227, pp. 65-72, 2016.
- [25] J. Huang, J. Zhou, Z. Liu, X. Li, Y. Geng, T. Xiaoqing, Y. Du, and Z. Qian, "Enhanced acetone-sensing properties to ppb detection level using Au/Pd-doped ZnO nanorod", *Sens. Actuator B Chem.*, Vol. 310, p. 127129, 2020.